

1      **Separation of an upwelling current bounding the Juan  
2      de Fuca Eddy**

3      **Jody M. Klymak<sup>1,2</sup>, Susan E. Allen<sup>3,4</sup>, Stephanie N. Waterman<sup>3</sup>**

4      <sup>1</sup>School of Earth and Ocean Sciences, University of Victoria, BC, Canada

5      <sup>2</sup>Department of Physics & Astronomy, University of Victoria, BC, Canada

6      <sup>3</sup>Department of Earth, Ocean and Atmospheric Sciences, University of British Columbia, Vancouver, BC,

7      Canada

8      <sup>4</sup>Institute of Applied Mathematics, University of British Columbia, Vancouver, BC, Canada

9      **Key Points:**

- 10     • The shelf break current along Vancouver Island separates downstream of a submarine  
11     bank.
- 12     • Offshore water is drawn onto the shelf and forms a sharp semi-persistent front with  
13     the Juan de Fuca Eddy.
- 14     • The Eddy shows evidence of long residence times, and little evidence of deep-water  
15     origin.

16 **Abstract**

17 Comprehensive water column observations of temperature, salinity, and oxygen on  
 18 the productive southern Vancouver Island shelf offer a unique characterization of processes  
 19 affecting exchange on the shelf. A semi-permanent cyclonic recirculation (the Juan de  
 20 Fuca Eddy) occupies the region in the lee of a bank where the shelf widens abruptly. The  
 21 observations indicate that the water in this Eddy is a mixture of offshore water and water  
 22 from a buoyant coastal current. The water in the in the Eddy is well-mixed along a mixing  
 23 line in  $\theta$ - $S$  space, though it retains stratification, and is either rapidly mixed (high  $\kappa$ ), or  
 24 has a long residence time (large  $\tau$ ), such that  $(\kappa\tau)^{1/2} \sim 50 - 100$  m. There is a sharp  
 25 temperature-salinity front on the offshore side of this well-mixed water, with the front  
 26 no more than 1-km wide, and no sign of instabilities. Previous work had hypothesized the  
 27 role of a spur canyon incising the shelf in feeding water to the Eddy; little evidence of this  
 28 was found during the observations, however, these were collected during a relaxation and  
 29 reversal of upwelling winds, which may have slowed the flow of water into the Eddy. Tidally  
 30 resolved observations in the spur canyon also show very strong hydraulic flows in the cross-  
 31 canyon direction accompanied by very high localized mixing rates in 50-m hydraulic jumps  
 32 possibly exceeding  $\kappa \sim 1 \text{ m}^2\text{s}^{-1}$ .

33 Upstream of the Eddy, there is an along-shelf current flowing equatorward with par-  
 34 tially mixed water properties compared to the well-mixed water in the Eddy. The shelf  
 35 current was observed to separate from the shelf in the lee of a bank, and is replaced by the  
 36 distinct offshore water mass that forms the offshore front with the Eddy. The separation  
 37 event can be seen in sea-surface temperatures in satellite images as tongue of water that is  
 38 ejected offshore, possibly with the relaxation of upwelling, with the flow heading directly  
 39 offshore. The cause of this offshore separation event is not determined, but likely involves  
 40 instability between the shelfbreak current and the California Undercurrent, and possibly is  
 41 catalyzed by separation from the abrupt underwater bank at the poleward end of the study  
 42 region.

43 **Plain Language Summary**

44 The southern Vancouver Island continental shelf is very productive due to high nutrient  
 45 input from the Strait of Juan de Fuca and Salish Sea estuarine system, and substantial cross-  
 46 shelf transport due to the complicated topography. The estuarine water flows poleward,  
 47 hugging the coast as the Vancouver Island Coastal Current, and in the summer shelf water  
 48 flows equatorward. Trapped between these two currents is the Juan de Fuca eddy, a stagnant  
 49 region of water that occupies the shelf where it abruptly widens just north of the Strait of  
 50 Juan de Fuca.

51 Here we present intensive sampling of the Juan de Fuca eddy region. The observations  
 52 show the eddy is low in oxygen, and we find has undergone substantial vertical and lateral  
 53 mixing. This indicates that the waters have a surprisingly long residence time for a coastal  
 54 feature, and that this region extends the depth of the water column. In contrast to previous  
 55 literature we find that the water likely has low oxygen from being used for respiration rather  
 56 than being pulled from deep in the California Undercurrent.

57 The sampling also shows a remarkable flow separation of the equatorward shelf current.  
 58 The current is shown to detach and is pushed offshore. Such events are readily seen in  
 59 satellite imagery, but the results here indicate that the separation extends the depth of the  
 60 water column on the shelf, and that this separation may be partially driven by the local  
 61 bathymetry. The separation is a very strong cross-shelf exchange event, and likely transports  
 62 substantial nutrient-rich coastal water offshore to drive productivity in the deeper ocean  
 63 adjacent to the continental slope.

## 64 1 Introduction

65 Cross-shelf exchange is important to the health and productivity of continental shelf regions,  
 66 where offshore oxygenated water is exchanged with nutrient-rich, but oxygen-depleted  
 67 nearshore water. Cross-shelf transport usually requires ageostrophic flow, since geostrophically  
 68 balanced flow will tend to follow topographic contours, often providing a barrier to  
 69 lateral exchange (Brink, 2016). Mechanisms for cross-shelf exchange include internal waves  
 70 and instabilities in shelf-break fronts. Most-dramatically, however, topography can drive  
 71 cross-slope exchanges, often seen most clearly in surface imagery, but occasionally observed  
 72 *in-situ* (Barth et al., 2000).

73 Here we present detailed *in-situ* observations from the southern Vancouver Island  
 74 shelf, collected in summer 2013, and sampled with a rapid profiling vehicle equipped with  
 75 a CTD and oxygen sensor, supplemented by traditional hydrographic surveys. The shelf  
 76 has complicated bathymetry figure 1, with a somewhat typical shelf poleward of our study  
 77 site, but then widening in the lee of La Perouse Bank, and then hitting the Juan de Fuca  
 78 canyon, equatorward. Water from the strait of Juan de Fuca flows poleward as a buoyant  
 79 current that hugs the coast (Thomson et al., 1989; Hickey et al., 1991), while shelf water  
 80 flows equatorward in the summer under upwelling conditions, both forced by local winds  
 81 and via tele-connections with the long, homogenous shelves equatorward off Washington and  
 82 Oregon (Hickey et al., 1991; Thomson & Krassovski, 2015; Engida et al., 2016). Trapped  
 83 between these two currents is a region of relatively homogenous water that has been termed  
 84 the Juan de Fuca Eddy (Freeland & Denman, 1982; Freeland & McIntosh, 1989; Foreman  
 85 et al., 2008; MacFadyen & Hickey, 2010).

86 A goal of our study was to understand how the Juan de Fuca Eddy persists, and  
 87 how it exchanges water properties with offshore water. Low oxygen has previously been  
 88 found in the Eddy, causing it to be inferred that water in the eddy is upwelled from as  
 89 deep as 400 m (Freeland & Denman, 1982; Dewey & Crawford, 1988). This inference was  
 90 based on the oxygen being conservative, and hence having to come from close to the oxygen  
 91 minimum zone found further offshore (Mackas et al., 1987) and lead to hypotheses that  
 92 perhaps the eddy was fed by waters being drawn up a spur canyon (called the Spur Canyon)  
 93 via ageostrophic transport from offshore to onshore due to the low pressure in the eddy  
 94 center (Weaver & Hsieh, 1987). Below, we will argue that there is not substantial evidence  
 95 of such transport, and that oxygen is likely low because of consumption due to respiration.

96 A second goal was to better understand cross-shore exchange with offshore water.  
 97 While the typical schematic of shelf exchange is that there are Ekman layers near the boundaries,  
 98 there is also evidence of filaments and wholesale separation of shelf currents into the  
 99 deep ocean, both at this site, and at others. Such events are important as they tend to  
 100 transport nutrient rich shelf water out into the open ocean, fueling offshore ecosystems.  
 101 Along the Vancouver Island shelf, large filaments or instabilities of the coastal current have  
 102 been inferred using satellite images (Ikeda & Emery, 1984; Thomson & Gower, 1998). Direct  
 103 observations of such filaments have been made further to the south off Cape Blanco (Barth  
 104 et al., 2000), and other coasts (Relvas & Barton, 2005, e.g.). Net cross-shore transport  
 105 of nutrients and chlorophyll have been found in hydrographic surveys off Vancouver Island  
 106 (Mackas & Yelland, 1999), and associated with mesoscale features both in geostrophic ve-  
 107 locities, and in satellite observations. The mechanisms driving such separations are poorly  
 108 understood, but hypotheses include coastal hydraulics (Dale & Barth, 2001) leading to  
 109 along-shore trapping of coastal waves, wind stress curl variations (Castelao & Barth, 2007),  
 110 induced relative vorticity due to stretching of parcels that inertially overshoot their initial  
 111 isobaths due to a sudden change in downstream bathymetry, and the non-linear breaking of  
 112 large-scale meanders due to baroclinic instability between the wind-driven current and the  
 113 California Undercurrent (Ikeda et al., 1984; Battean, 1997).

114 In this paper we present observations from 2013 (section 2), presenting the data in  
 115 a number of ways to highlight the important processes, with a focus on the offshore side

116 of the eddy region (section 3) where we consider the age of the eddy, the steadiness of the  
 117 front separating the eddy and the offshore water, properties along the spur canyon that  
 118 was believed to feed the eddy, and finally describe a large offshore tongue of the shelf-  
 119 break current and its intrusion into the interior. We discuss the origin of the eddy and the  
 120 implications of the separating jet (section 4).

## 121 2 Site and Methods

122 Observations from three summer cruises in 2013 are discussed here. Two were hydro-  
 123 graphic surveys carried out on the *CCGS Tully*, one in June, and the other in late  
 124 September. The third was a finescale survey made in the Vancouver Island shelf between 21  
 125 and 30 August 2013, aboard the *R/V Falkor*. The study site was the southern portion of the  
 126 Vancouver Island Shelf (figure 1a), a particularly complicated region due to the bathymetry  
 127 and varied forcing.

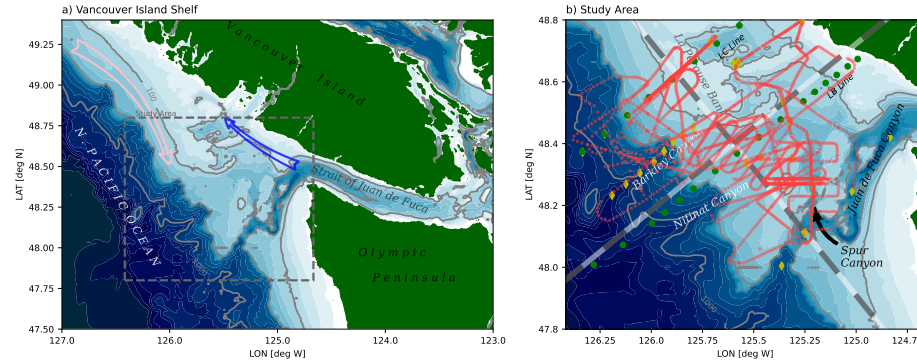


**Figure 1.** a) Study site on the Vancouver Island Shelf. The blue arrow indicates the direction of the Vancouver Island Coastal Current. The pink arrow indicates southward flow of the coastal upwelling current. The dashed box indicates the approximate limits of the study area. b) The study area with hydrographic casts from the La Perouse cruises along the LB and LC Lines are green dots, hydrographic casts during the Falkor cruise indicated in yellow dots, and Moving Vessel Profiler casts as red dots. The coordinate system used for this paper is shown with alternating grey and white bands at 10-km intervals.

128 At the south end of the study site is the Juan de Fuca canyon, which feeds dense water  
 129 into Juan de Fuca Strait. This dense water is mixed with fresh water from the Fraser River  
 130 at the sills and archipelagos further inland, and fluxes out the Strait again, where it turns  
 131 poleward along Vancouver Island to form the Vancouver Island Coastal Current. The Juan  
 132 de Fuca Canyon has a notable spur canyon (Spur Canyon), that incises the shelf towards  
 133 the north into the study site (figure 1b). The rest of the shelf is punctuated by a series of  
 134 banks and shallow basins. Notable is La Perouse bank, running along the shelf from the  
 135 north, and moving isobaths offshore until it abruptly ends at around 48.5 N. The shelf break  
 136 is characterized by a series of submarine canyons, in particular Nitnat Canyon and Barkley  
 137 Canyon.

138 We consider routine hydrographic surveys along the LB and LC lines, collected aboard  
 139 the *CCGS Tully* from 2013-05-30 to 2013-05-31 (“June”), and 2013-09-07 to 2013-09-09  
 140 (“September”). These lines span the depths from about 50 m to deep offshore, with casts  
 141 every 7.5 km across shelf. The data comes from a lowered Seabird 9-11 CTD, with an  
 142 SBE 43 oxygen sensor. Oxygen data have been checked against bottle casts, and the CTD  
 143 corrected for sensor offsets and thermal lags.

We focus on fine-scale surveys carried out from 2013-08-21 to 2013-08-30. Data were collected from the *R/V Falkor* with an ODIM Brooke-Ocean Moving Vessel Profiler (MVP). The MVP was equipped with an AML Oceanographic CTD, and a Rinko Oxygen sensor with a 7-s response time foil. The MVP profiles to depths of 200 m or to within 5 m of the seafloor, whichever is shallower, and drops at a speed of  $3 \text{ m s}^{-1}$ . Data collection took place while the ship cruised at speeds between 5 and 8 kts, usually at around 6 kts to enable fine horizontal spacing of the casts, with typical spacing less than 800 m. Data is reported for the downcast, which mostly follows a vertical path. The rapid speed of the profiling makes the oxygen measurements somewhat coarse, and probably biased due to the phase lag of the sensor, so we treat these largely qualitatively in this paper.

Unfortunately, neither vessel had an operational acoustic Doppler profiler during the cruises with which to make current measurements.

Winds during the cruises were typical for the west coast of Vancouver Island, with upwelling favorable winds during July and early August (figure 2). During the finescale cruise, and for the week previous, the winds were intermittently downwelling favorable. Note that this locale is strongly affected by coastally trapped waves from further south, so doming of near-bottom isopycnals often persists despite local wind forcing (Thomson & Krassovski, 2015; Engida et al., 2016), and takes a finite amount of time to spin down.

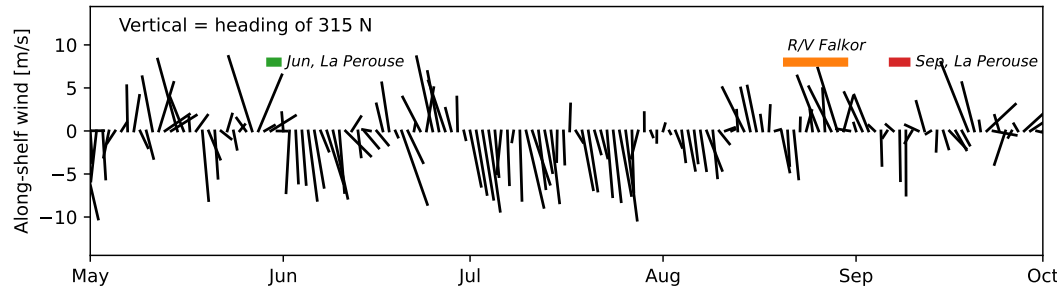


**Figure 2.** Wind from the La Perouse buoy (DFO, 2022). The vertical direction is along-shelf (chosen as a heading of 315 N), so vectors pointing straight down represent upwelling winds. The wind components has been low-pass filtered to one-day averages. The timing of the cruises discussed in the paper are shown as colored bands.

### 3 Observations

#### 3.1 Early and late summer broad-scale surveys

Hydrographic sections along the LB and LC lines highlight summer conditions on the Southern Vancouver Island Shelf, and indicate some of the features we are focusing on in this paper (Figure 3). During both cruises and at both lines there is clear evidence of upwelling, with the  $26.4 \text{ kg m}^{-3}$  isopycnal reaching from 130 m depth to shallower than 85 m over the shelf. This dense water tends to be low in oxygen and cool. Further onshore, isopycnals tilt back down, and the water warms, evidence of the Vancouver Island Coastal Current that hugs the coast here.

The Juan de Fuca Eddy region is along the LB Line (figure 3, bottom three rows), mostly inshore of 0 km. This water is cooler and lower in oxygen than along the same isopycnal further offshore. Also note that during the June cruise the water in this region was cooler and more oxygenated than later in the summer during the September cruise.

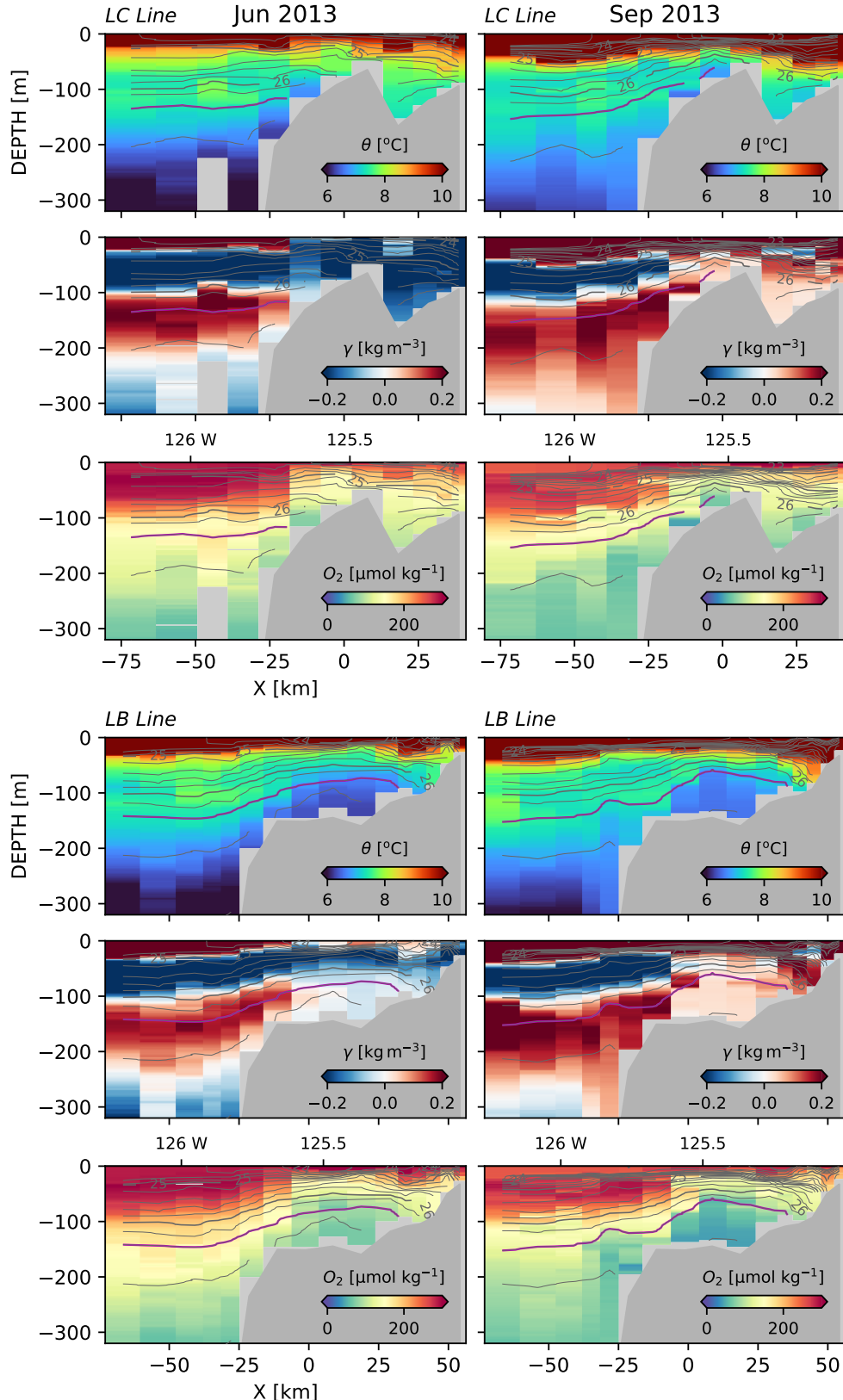


**Figure 3.** Observations along LC (top three rows) and LB lines (bottom three rows) in Jun (left column) and Sep 2013 (right column). X is across-shelf distance in the coordinate system shown in figure 1. Potential density is contoured every  $0.2 \text{ kg m}^{-3}$ , with the  $26.4 \text{ kg m}^{-3}$  colored magenta. Potential temperature,  $\theta$ , spice anomaly,  $\gamma$  and oxygen concentration,  $O_2$ , are colored for each section.

Near the surface, the isopycnals are domed, but the low-oxygen anomaly extends as high as the thin surface mixed layer.

The water upstream of the Eddy region, along the LC line appears less mixed than the Eddy water. It does not show as much drawdown of oxygen, and is warmer, at least offshore of La Perouse bank (figure 3, top three rows). Water does not appear to make it over La Perouse bank into the basin onshore, or if it does, it does so intermittently. There appears to be some mixing of the deeper and shallow water near  $26.4 \text{ kg m}^{-3}$ , with the water along this isopycnal becoming cooler and lower in oxygen where it intersects the shelf, consistent with enhanced mixing near the shelf

The  $\theta$ - $S$  properties show many of the features demonstrated above (figure 4a). Below  $26.6 \text{ kg m}^{-3}$  or so, the deep water masses are found offshore, and are largely homogenous. Shallower, there are distinct differences between the water found offshore, with it being warmer and saltier than water on the shelf at the same densities. These anomalies are hard to parse directly, so in this paper we use a spice anomaly, relative to a straight line in  $\theta$ - $S$  space (figure 4). This line represents an approximate mixing line for water in the Eddy, and passes the points  $7.75^\circ\text{C}$ ,  $30 \text{ psu}$  and  $6.6^\circ\text{C}$ ,  $35 \text{ psu}$ . Spice anomaly for a given water sample at density  $\sigma_\theta$  is given by  $\gamma = \alpha(T - T_0(\sigma_\theta)) + \beta(S - S_0(\sigma_\theta))$  where  $T_0(\sigma_\theta)$ , where  $S_0(\sigma_\theta)$  are the temperature and salinity along the mixing line at the same density as the water sample, with the sign convention that positive is warmer and saltier than data along the mixing line.

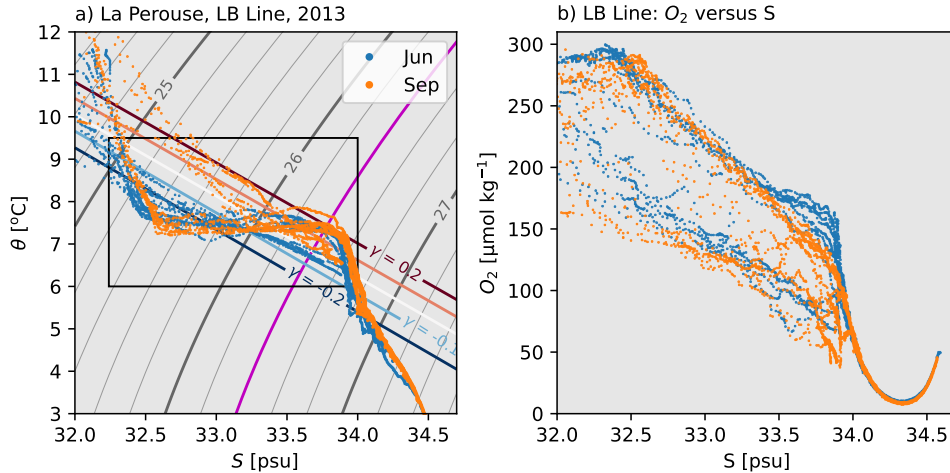


**Figure 4.** Potential temperature versus salinity for the La Perouse data shown in figure 3; potential density is contoured every  $0.2 \text{ kg m}^{-3}$ , with the  $26.4 \text{ kg m}^{-3}$  colored magenta. A definition of spice anomaly is shown in this plot, and discussed in the text. The rectangle is the  $\theta$ - $S$  range used in figure 5 below.

Offshore water tends to be high in absolute spice anomaly (figure 3, middle rows), with a positive-anomaly layer (red) centered at  $26.4 \text{ kg m}^{-3}$  sandwiched between negative-anomaly layers above and below. On the shelf ( $-10 \text{ km} < X < 30 \text{ km}$ ), the distinct  $\theta$ - $S$  masses are attenuated and much closer to the defined mixing line than the offshore water (closer to white in color). Hugging the coast ( $X > 30 \text{ km}$ ), is the Vancouver Island Coastal Current, with a negative spice anomaly in June, and a positive anomaly in summer, consistent with seasonal warming.

The June and September cruises are quite similar in water properties, particularly in the offshore waters. Water has upwelled from deeper depths in September, but has most

204 of the same water mass characteristics as earlier in the year. The water on the shelf is  
 205 somewhat warmer than earlier in the year, and by September has started to fall off the  
 206 mixing line.

207 In terms of oxygen, both cruises have a similar dichotomy between the onshelf and  
 208 offshelf water, with water found in the eddy tracking at least  $100 \mu\text{mol kg}^{-1}$  lower on the  
 209 shelf than offshelf (figure 3, figure 4b). The very deepest water ( $S \approx 33.9 \text{ psu}$ ) on the shelf  
 210 shows a further  $50 \mu\text{mol kg}^{-1}$  drop between June and September along the LB line.

### 211 3.2 Fine-scale surveys

#### 212 3.2.1 Overview

213 As shown in figure 1, we conducted a large spatial survey of the shelf using the Moving  
 214 Vessel Profiler, collecting over 2000 CTD casts in a relatively synoptic manner. This amount  
 215 of data allows a reasonable census of the water masses that motivated our choice of the  
 216 mixing line shown in figure 4. Binning in temperature and salinity, we can look at sample  
 217 frequency of these observations figure 5, and we see that there are distinct water masses with  
 218 few observations between them. Looking along the  $26.4 \text{ kg m}^{-3}$  isopycnal, we see that there  
 219 is a large population along the mixing line. At the opposite extreme, we see that there is  
 220 a large population with a positive spice anomaly of approximately  $0.2 \text{ kg m}^{-3}$ , representing  
 221 the offshore water. Between these two end points there is a third water mass, somewhat  
 222 indistinct from the offshore water mass, but very distinct from the water mass along the  
 223 mixing line. These three water masses exist on deeper and shallower isopycnals as well,  
 224 but become hard to distinguish from  $\theta - S$  properties alone as the properties converge near  
 225  $26.1 \text{ kg m}^{-3}$ .

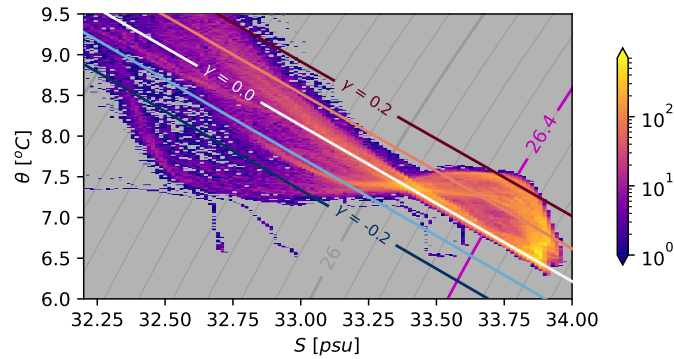


**Figure 5.** Sample density of salinity and potential density data from the cruise, with a logarithmic color scale. Grey contours are potential density relative to the surface, every  $0.1 \text{ kg m}^{-3}$ , and the magenta contour is the  $26.4 \text{ kg m}^{-3}$  isopycnal. Spice anomaly,  $\gamma$ , is defined as temperature anomaly scaled by the thermal expansion co-efficient,  $\alpha$ , along isopycnals from the mixing line found in the well-mixed region in the Eddy (white line), in  $\text{kg m}^{-3}$ .

226 In synthetic cross sections of spice anomaly, the Eddy is clearly identifiable as water  
 227 that is along the straight mixing line, and thus has low-spice anomaly ( $\gamma \approx 0 \text{ kg m}^{-3}$ ,  
 228 figure 6c, d). This signature of well-mixed water extends from the seafloor to approximately  
 229 30 m depth, onshore of  $x \approx 0 \text{ km}$ . Despite lying along a mixing line, the Eddy water is still  
 230 stratified. This well-mixed water contrasts with water directly offshore on the other side  
 231 of a sharp  $\theta - S$  compensated front that is warmer and saltier than the well mixed water

( $\gamma > 0.2 \text{ kg m}^{-3}$ ) deeper than  $26 \text{ kg m}^{-3}$ , and colder and fresher shallower. The thickness of this front is even sharper in individual sections than in these composite sections (see section 3.2.2).

In contrast, the third population of partially mixed water mass identified in figure 5 is all found upstream of the Eddy region (figure 6a, b) as a weaker spice anomaly ( $\gamma \approx 0.1 \text{ kg m}^{-3}$ , “pink” colors). This water is generally found near the intersection of the upwelling water and La Perouse Bank, and is not as warm as offshore water, indicating some mixing has taken place. Of note, is that this intermediate water mass appears completely absent in the sections further equatorward (figure 6c, d), indicating that it is either mixed away, or that it is advected elsewhere; we argue below that it is advected offshore in a large-scale tongue.

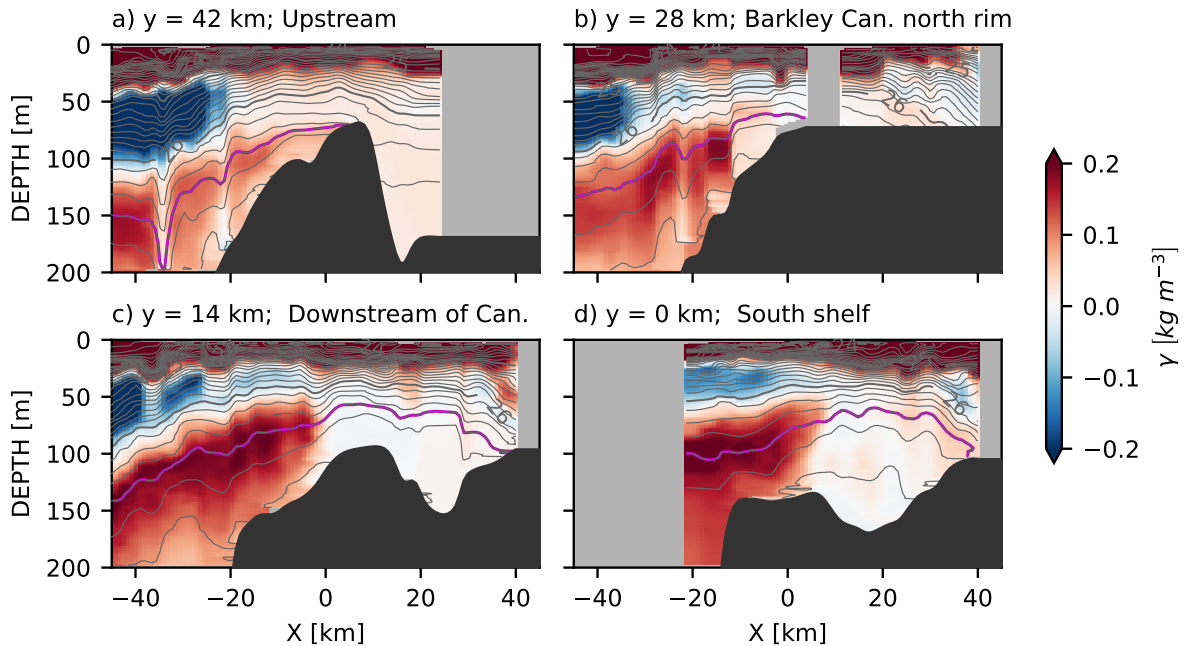


**Figure 6.** Synthetic sections of spice anomaly from the MVP data, projected along four lines from poleward (upstream of coastal current) a) to equatorward (downstream); the lines are shown in figure 1b). Isopycnals are contoured every  $\sigma_\theta = 0.2 \text{ kg m}^{-3}$ , with the  $\sigma_\theta = 26.4 \text{ kg m}^{-3}$  isopycnal highlighted in magenta. Colors are spice anomaly as defined in figure 5. ”BC” in panel (c) refers to Barkley Canyon.

Oxygen section show similar trends, with the low-spice anomaly water having low oxygen saturations, while the strong negative spice anomaly shallower than  $\sigma_\theta = 26.4 \text{ kg m}^{-3}$  has very high oxygen, and the deeper water is also more oxygenated. Of note is that compared with the coarser sampling along the LC Line (figure 3), we see that the abrupt transition between offshore and Eddy water is also present in oxygen.

The spatial patterns are very clear when considering a map-view of properties along the  $\sigma_\theta = 26.4 \text{ kg m}^{-3}$  isopycnal (figure 8). There is a region onshore of the south tip of La Perouse Bank (approximately 44.5 N, 125.75 W), that consists of water that is found along the mixing line (spice anomaly  $\gamma \approx 0 \text{ kg m}^{-3}$ ) with low oxygen saturations. Offshore of this region is water that is very warm and salty in comparison ( $\gamma > 0.15 \text{ kg m}^{-3}$ ), and relatively high in oxygen (saturations of approximately 60%). The region between these two water

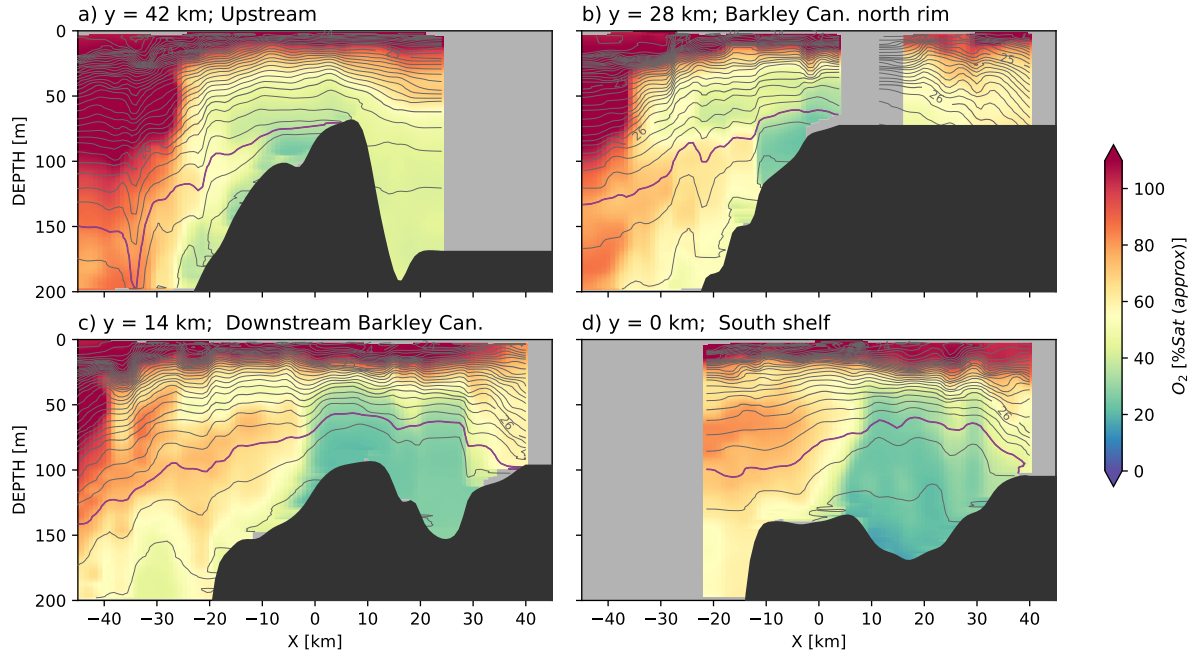


**Figure 7.** Synthetic sections of Oxygen, approximate percent saturation from the MVP data.

masses is very abrupt, and is concave with respect to the isobaths on the shelf, stretching from La Perouse Bank to a shallow bank just above the Juan de Fuca canyon (48.3 N and 125.4 W).

Upstream of La Perouse bank and Barkley Canyon, the water along the shelf the weaker spice anomaly of the third water mass ( $\gamma \approx 0.1 \text{ kg m}^{-3}$ , light pink colors). This water is also somewhat lower in oxygen than water from offshore, though not as depleted as the water in the Eddy. This water appears to be pushed offshore just upstream of Barkley Canyon, and replaced on the shelf by the warmer offshore water.

### 3.2.2 Frontal survey

A systematic survey through the front between the offshore water and the Eddy water demonstrates the structure of the front (figure 9). The survey started close to shore and passed through the Vancouver Island Coastal Current (along-track 0-10 km). The coastal current water is buoyant and significantly fresher and cooler than water at the same density near the surface and forms a classic density front with

The front between the offshore water and the “eddy” water was passed through 10 times, showing its evolution following the along-shore equatorward flow. First, as noted in the composite sections, isopycnals slope up from offshore onto the shelf. This is in agreement with a shelf-break current, though the isopycnals flatten out in the Eddy region. The front starts out very sharp, (along-track distance 50 km) though two small tendrils can be seen separating from the front on the inshore side. Similar tendrils are found on the second pass, perhaps a bit more separated from the front ( $\approx 80 \text{ km}$ ), and on the third pass ( $\approx 95 \text{ km}$ ). Note that these tendrils are made of up partially mixed water. The subsequent passes have more of this partially mixed water, such that the partially mixed region is up to 5-km wide by the fifth pass ( $\approx 150 \text{ km}$ ). However, note that the deeper isopycnals retain a sharp front, and indeed the front appears sharp again by the seventh pass at all depths.

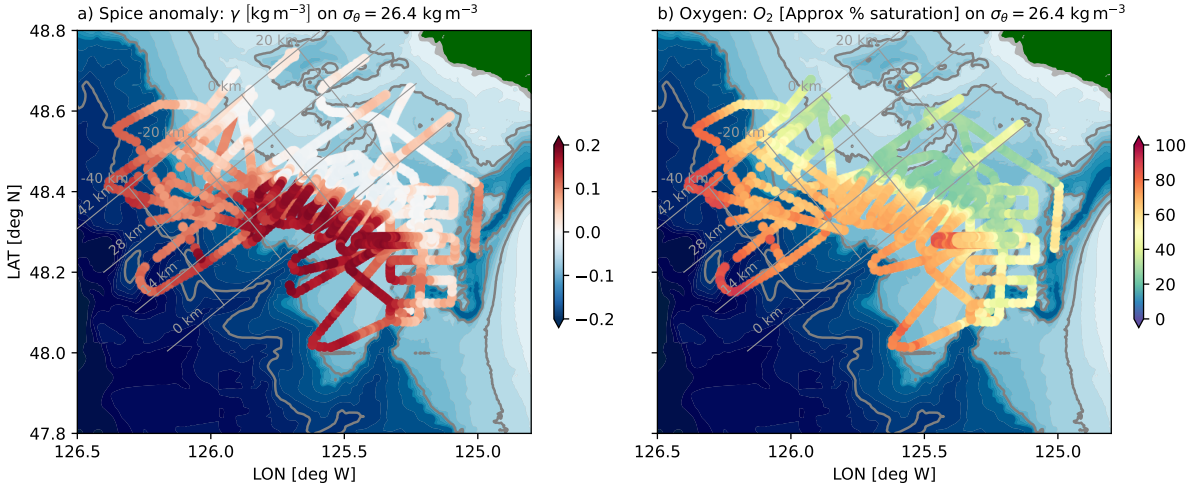


**Figure 8.** Spatial overview of a) local spice (temperature anomaly on an isopycnal: see text), and b) oxygen saturation on the  $\sigma_\theta = 26.4$  kg m $^{-3}$  isopycnal. Grey cross-slope lines are cross sections indicated in figure 6. Along-slope grey lines are every 20 km in the cross-slope direction, with  $x = 0$  km near the 100-m isobath at the north end of the observation area.

There is evidence of some warmer water swirling into Eddy, particularly along isopycnals deeper than 26.4 kg m $^{-3}$ . Regions of warmer (and more oxygenated) water are found in tendrils at these depths (e.g.  $\approx 170$  km and  $\approx 185$  km).

The overall effect is similar to what was seen in the Gulf Stream with similar observations (Klymak et al., 2016); there are two quite distinct water masses, the Eddy water and the offshore water, as seen in the  $\theta$ -S plot (figure 9c). There is only a small population of samples between these two, indicative of substantial isopycnal and vertical mixing, but even these populations are relatively cut off from the main water masses, indicating that they are well-mixed on their own, in short episodic events.

### 3.3 Spur Canyon

The Spur Canyon leading from the Strait of Juan de Fuca has been implicated in allowing dense water to be upwelled into the Eddy. The seafloor is low in the middle of the Eddy, so water has been hypothesized to move up the Spur Canyon due to ageostrophic motion (Weaver & Hsieh, 1987; Freeland & Denman, 1982). This is difficult to infer from water properties alone. Three transects up the canyon indicate that deep isopycnals slope up into the canyon (figure 10, to approximately 30 km). Across the eddy, isopycnals are largely flat until they intersect the Vancouver Island Coastal Current ( $x \approx 80$  km). The deeper isopycnals do not make it into the deeper basin northeast of La Perouse bank ( $x \approx 70$  km).

Water properties along the canyon go from offshore water, to Eddy water. Oxygen behaves in a similar manner, though some of the incoming water has slightly lower oxygen than water inside the eddy (not shown). Based on these sections, it is difficult to infer water motion up the canyon in particular.

Much of the modified water in the Spur Canyon appears to come from the shelf to the west, but heavily modified by tidal mixing. A repeated tidal survey over the bank on the west side of the canyon shows a strong hydraulic response (figure 11) during onshore flow (17:58–21:00). Dense ocean water passes from the offshore side into the Canyon, and

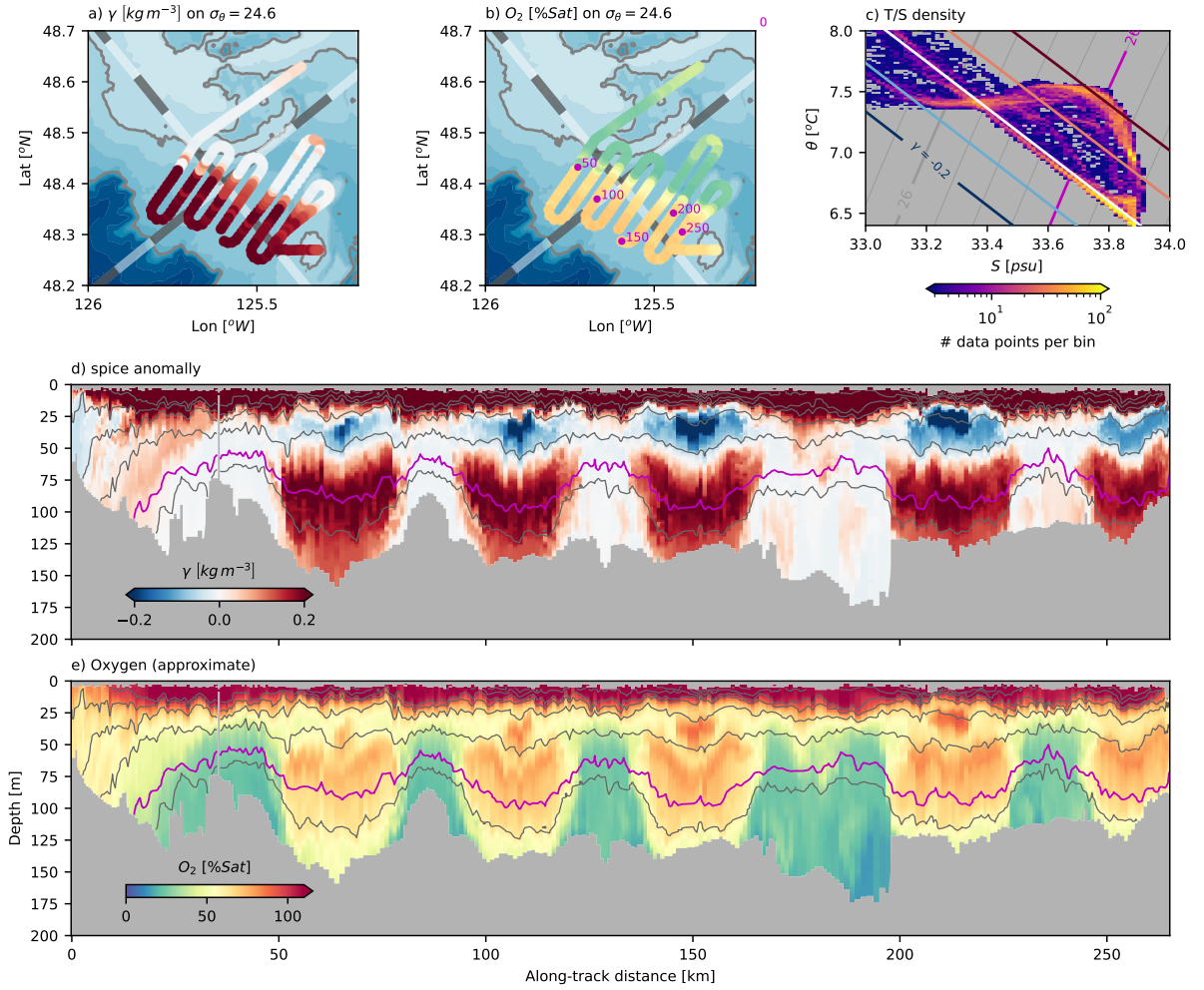


**Figure 9.** Data from a survey focusing on the front region (2013-08-28T15:11 to 2013-08-29T09:18) a) spice anomaly along  $26.4 \text{ kg m}^{-3}$ . Grey-white alternating lines are the coordinate system, with 10-km alternating shades. b) oxygen saturation; magenta dots correspond to distance along-track. c) density of data points (logscale) in this section of data. d) cross-section of spice anomaly along track. Grey isopycnals are contoured every  $0.5 \text{ kg m}^{-3}$ , and the  $26.4 \text{ kg m}^{-3}$  isopycnal is shown in magenta. e) cross-section of oxygen saturation.

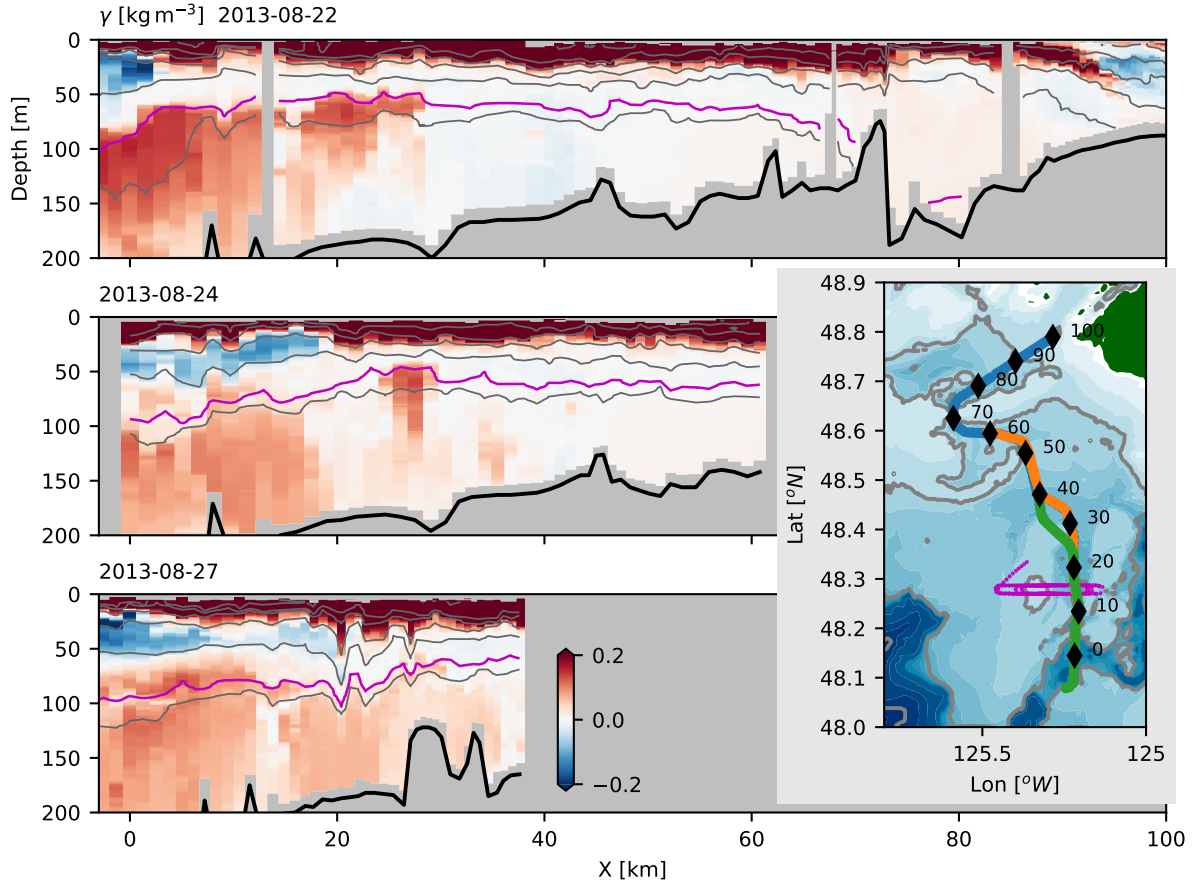


**Figure 10.** Three surveys up the Spur Canyon, where  $X$  is along-canyon as defined in the map. Grey isopycnals are contoured every  $0.5 \text{ kg m}^{-3}$ , and the  $26.4 \text{ kg m}^{-3}$  isopycnal is shown in magenta. The seafloor is indicated with the thick black line. Map shows the path taken during each survey in chronological order blue, orange, and green. Magenta line is path taken during a cross-canyon survey (figure 11).

305 plunges down the side wall before rebounding downstream. Note that the tide here is  
 306 largely diurnal, so this onslope flow only occurs once a day. Given the stratification of  
 307  $N \approx 6 \times 10^{-3} \text{ rad s}^{-1}$  and an overturning scale of 50 m, we might expect dissipation rates  
 308 reaching  $\epsilon \sim L^2 N^3 \approx 5 \times 10^{-4} \text{ m}^2 \text{s}^{-3}$ , which is more than three orders of magnitude higher  
 309 than dissipation observed west of this location by Dewey and Crawford (1988). In terms of  
 310 a diapycnal diffusivity  $\kappa = \gamma \epsilon / N^2 \approx 1 \text{ m}^2 \text{s}^{-1}$ , assuming a mixing efficiency of  $\gamma = 0.2$ . The  
 311 effect on the properties in the canyon is for water to spill over from the offshore front into  
 312 the canyon during the tide. This water is rapidly mixed with surrounding water such that  
 313 its strong offshore spice values are attenuated.

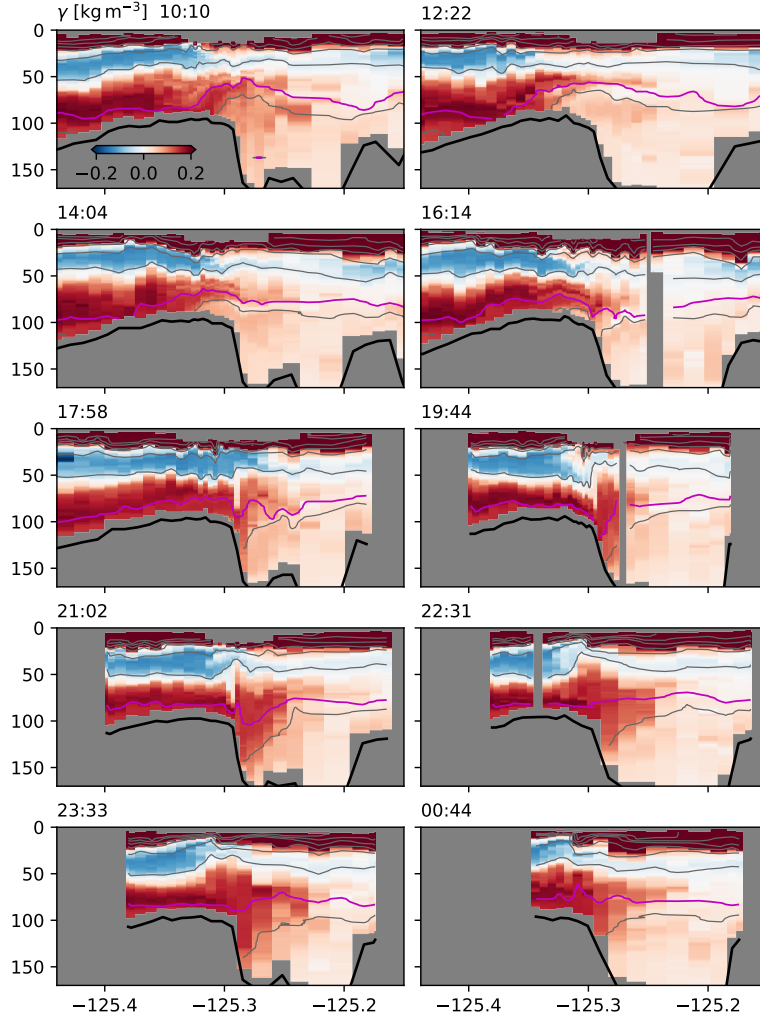


**Figure 11.** Repeated, tide-resolving survey across the Spur Canyon, time is indicated in the upper left of each plot (29 August, 2013). See magenta line on map figure 10 for location of survey.

314 This cross-canyon mixing makes it ambiguous if there is water moving up the canyon  
 315 or not. There is indeed a general tendency along the canyon for higher spice water to be  
 316 found offshore (figure 10) but it seems likely the source of the higher spice is over the bank  
 317 rather than water being advected up the canyon.

### 318 3.4 Offshore tongue

319 As discussed above, the very sharp T/S front between the well-mixed Eddy water and  
 320 the offshore water persists, despite there being considerable partially-mixed water found  
 321 upstream along the shelf. The partially-mixed water must go somewhere, and indeed it  
 322 appears to largely be pushed offshore just upstream of Barkley Canyon (figure 12). There  
 323 is a tongue of partially mixed ( $\gamma$  is pink along  $26.4 \text{ kg m}^{-3}$ ) that flows almost due south just  
 324 west of 126 W. We had trouble crossing the whole tongue with the scale of our surveys, but  
 325 it is at least 30 km wide. It also appears to end at approximately 48.2 N. This partially  
 326 mixed water reaches from relatively shallow isopycnals to at least  $26.6 \text{ kg m}^{-3}$  (figure 12, left  
 327 panel). Unfortunately, we cannot track the fate of this water mass because isopycnals tilt  
 328 down offshore, below the depth limit of the MVP. The shallower isopycnal appears to have  
 329 the tongue closer to the shelf than at  $26.4 \text{ kg m}^{-3}$ , indicating strong three-dimensionality to  
 330 this feature.

331 This feature is embedded in the larger scale isopycnal tilt caused by the upwelling  
 332 (figure 12 right panels), so it is difficult to see dynamically what is driving this offshore  
 333 push. One possibility is that it is simple flow separation as the water is not able to make  
 334 the sharp turn around La Perouse Bank. Whatever causes it, downstream of the separation,  
 335 the water is replaced by offshore water with much higher spice values.

336 There is a clear surface expression of the separating tongue in satellite imagery (fig-  
 337 ure 13). Water flowing equatorward along the shelf tends to be cooler than offshore water,  
 338 likely mixing with the colder coming out of the Strait of Juan de Fuca. On Aug 25, there is a  
 339 cold tongue of water separating from La Perouse bank, crossing isobaths and pointing south  
 340 at 125.8 W. There is cooler tendril streaming west at 48 N off the south end of this tongue.  
 341 This feature is not as well-developed in the previous image, Aug 21, perhaps indicating that  
 342 it is an evolving feature. By 31 Aug, there is no surface expression of the feature, though  
 343 small tendrils of cooler water can be seen separating from La Perouse Bank. By Sep-05 the  
 344 water has significantly warmed, but the offshore anomaly does not appear to have a surface  
 345 signature.

346 Satellite-based surface chlorophyll estimates show the same feature (figure 14) demon-  
 347 strating the advection of high chlorophyll to the west side of the Eddy. It also shows a rela-  
 348 tively high-chlorophyll tendril to the west, again exiting the study region at approximately  
 349 48 degrees N. The feature is relatively long-lived, on the order of one month. Inspection  
 350 of images before 2013-08-05 were too obscured by clouds, or did not show this feature. By  
 351 2013-09-06, we see the feature fading from the satellite. However, note that this feature is  
 352 centered 0.2 degrees of latitude south of tongue that we observe deeper in the water column,  
 353 again indicating that there is some depth-dependence to the feature.

## 354 4 Summary and Discussion

355 The intensive sampling discussed here has demonstrated a few important features of  
 356 the South Vancouver Island Shelf. First, there is a sharp and persistent temperature-salinity  
 357 compensated front between offshore water, and water that has been termed Eddy water.  
 358 This is readily determined in  $\theta - S$  space, with the Eddy water lying along a straight mixing  
 359 line, and the offshore water having a sharp kink centered at  $26.4 \text{ kg m}^{-3}$ . Second, there was  
 360 not strong evidence of water moving up the Spur Canyon during our observations, but the  
 361 Spur Canyon was a site of hydraulic cross-canyon flows in which we infer significant mixing.  
 362 Finally, upstream of the Eddy region water in the equatorward shelf current is partially  
 363 mixed in  $\theta - S$  space, and is seen to separate from the shelf at the point of an abrupt bend  
 364 in an underwater bank. The water mass crosses isobaths and is ejected into the interior; this  
 365 can also be observed from satellites. Thus the water that is offshore of the Eddy appears to  
 366 have been brought onto the shelf in exchange with this offshore tongue.

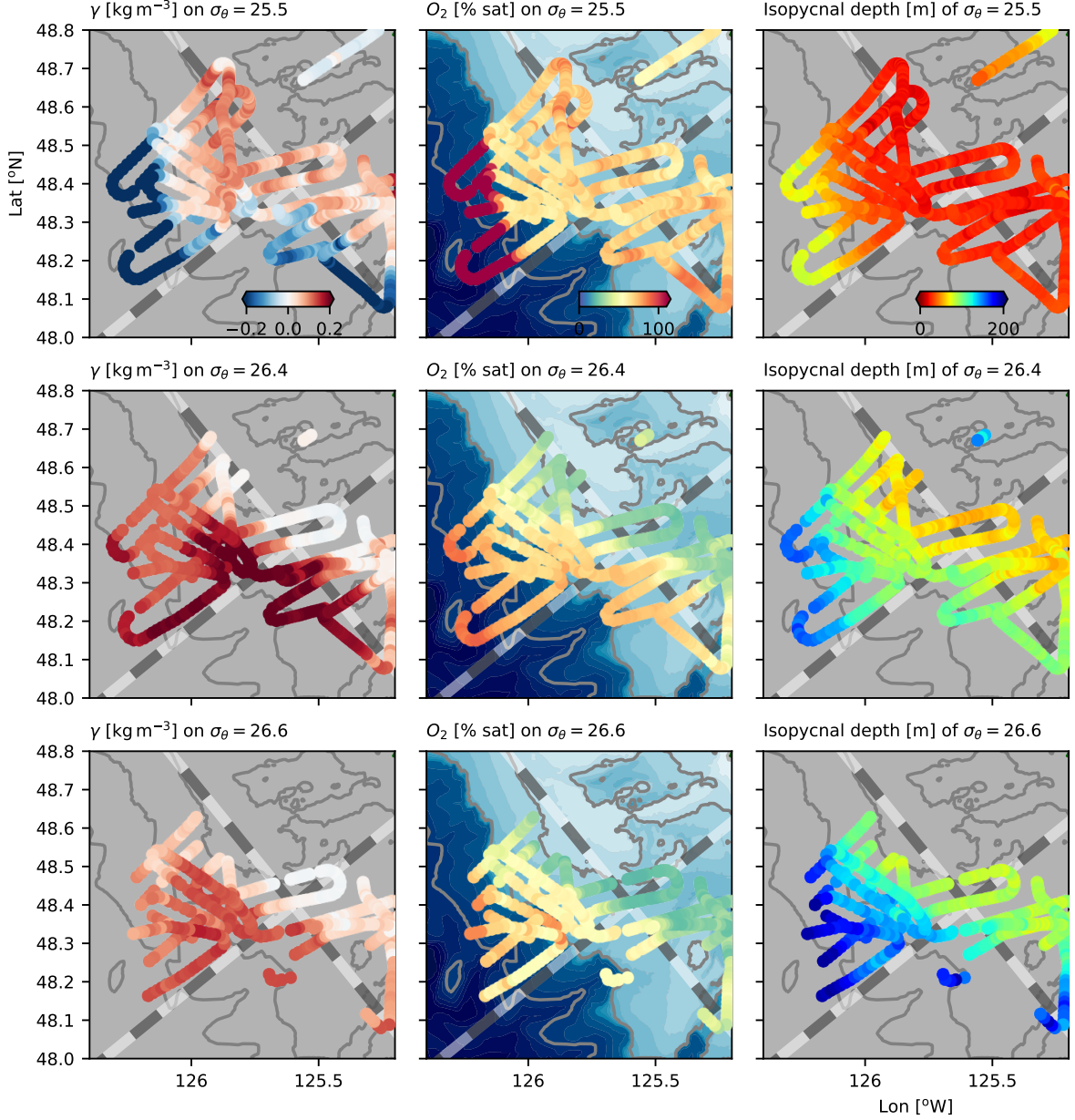


**Figure 12.** Isopycnal slices through showing the vertical structure of the water separating from the shelf, with the first row along  $25.5 \text{ kg m}^{-3}$ , second along  $26.4 \text{ kg m}^{-3}$ , and the third at  $26.6 \text{ kg m}^{-3}$ . First column is the spice anomaly, second is oxygen saturation, and the last column is depth of each isopycnal.

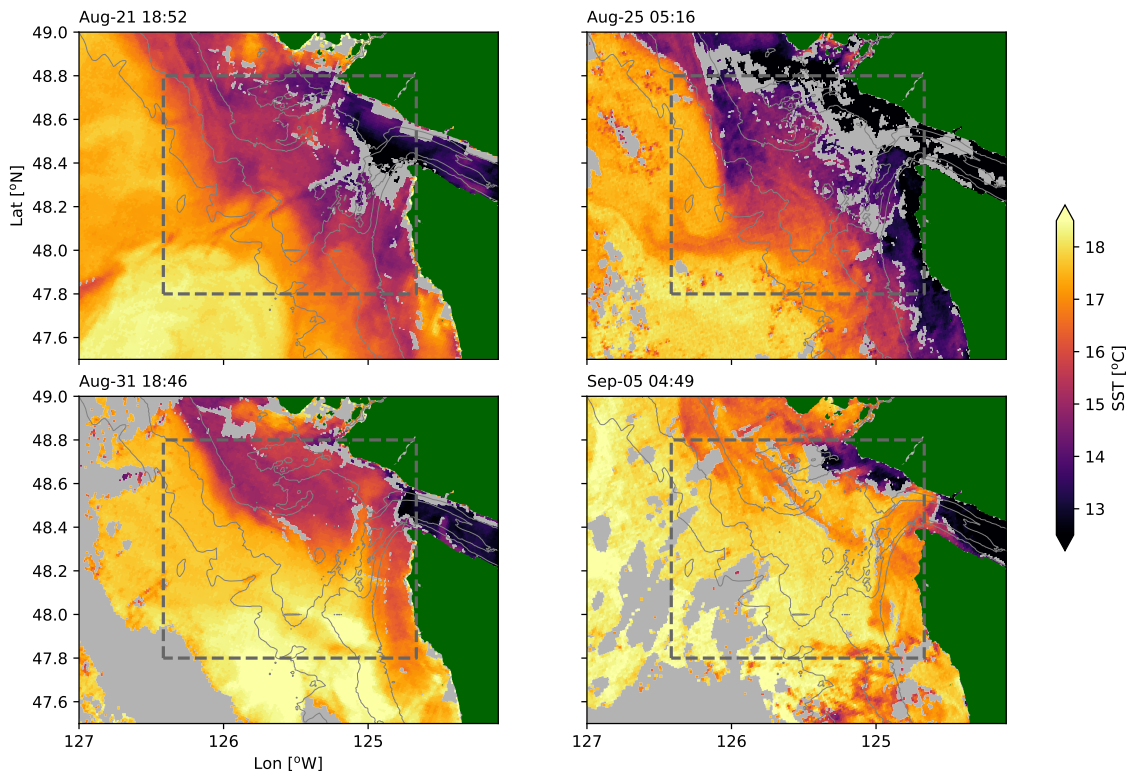


**Figure 13.** Sea surface temperature snapshots from the observation period. Grey areas are clouds; dashed gray line is the study area. Depths are contoured in thin gray lines at 200, 150 and 100 m. (OSI SAF, 2015)

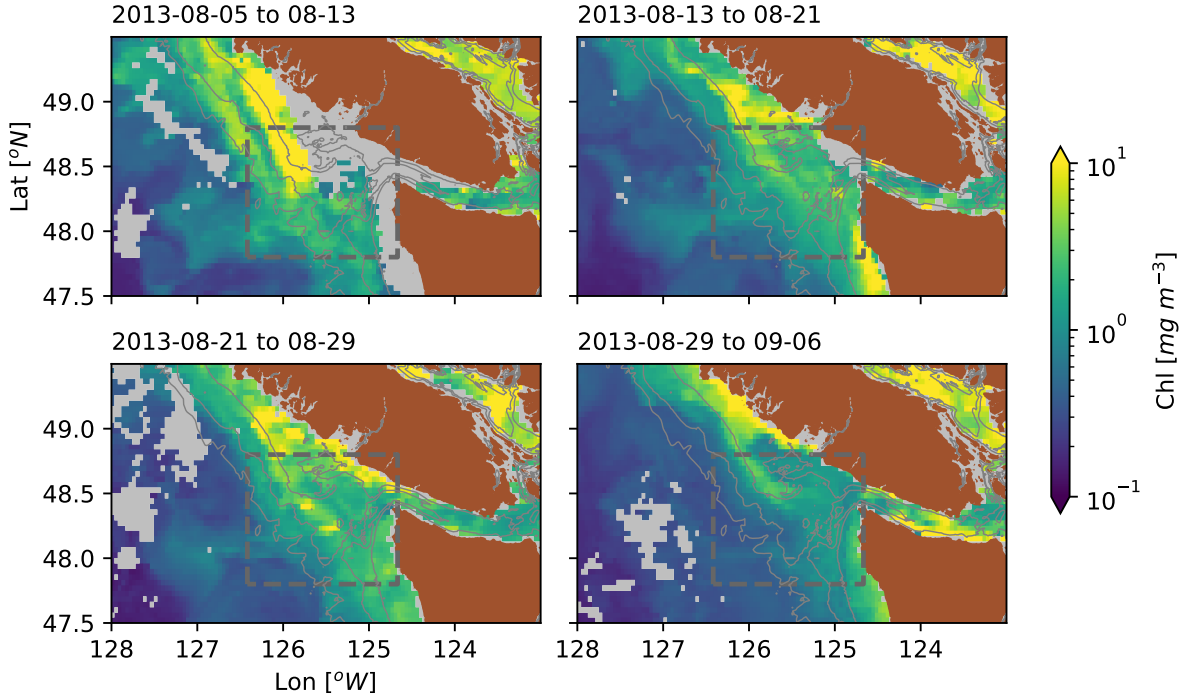


**Figure 14.** Surface chlorophyll density estimated from ocean color (Hu et al., 2012; NASA Ocean Biology Processing Group, 2017) over 8-day windows in 4-km bins. Gray regions had too many clouds for acceptable averages.

#### 4.1 Age and source of the eddy water

The source of water and formation of the Juan de Fuca Eddy has received substantial attention, however, the observations of a tight mixing line in  $\theta$ - $S$  space presented here are a new observation. The deepest water in the eddy could originate along the  $\theta$ - $S$  line from approximately 5.5 degrees to 7.5 degrees (figure 4a), which in the open ocean spans depths from 420 m to 70 m. Mackas et al. (1987) attempted to determine the origin of the water by including oxygen as a third variable to resolve the ambiguous  $\theta$ - $S$  relation. However, as figure 4b makes clear, oxygen is definitely not a conserved property in the eddy, with concentrations up to  $150 \mu\text{mol kg}^{-1}$  lower in the eddy than the water found offshore, and in a way that definitely cannot result from conservative mixing. As a best guess, if the water in the deepest part of the eddy came from a vertical mixture of the water at  $26.5 \text{ kg m}^{-3}$  and an equal distance down in density space of  $26.7 \text{ kg m}^{-3}$ , then the deepest water in the eddy would be coming from a depth of 250 m. This is a typical upwelling depth for coastal flows, and may not require extra input up Spur canyon as posited by Freeland and Denman (1982).

We found little evidence of vigorous flow up the Spur Canyon, or if there is, then the mixing in the canyon is quick enough to remove the  $\theta$ - $S$  signature of offshore water within 20 km of the canyon mouth (figure 10). We did find substantial evidence of mixing in the canyon, but the primary route of high-salinity water into the canyon appears to be due to tidal flow over the banks on the west side (figure 11), rather than evidence of flow up the canyon. However, it is also of note that upwelling winds had ceased at this point (figure 2), meaning that the offshore surface pressure gradient may be reduced, leading to reduced ageostrophic upwelling in the canyon. Whether the cessation of winds would also lead to a reduction of the low sea level height in the center of the eddy is an open question.

391 There is evidence of aging of the water in the eddy between late spring and late summer  
 392 (figure 3), with a reduction of oxygen in the eddy. If we posited that the reduction was all in  
 393 the same water, then the oxygen consumption rate over the time between the late-May and  
 394 early September cruises would be on the order of  $0.5 \mu\text{mol kg}^{-1}\text{d}^{-1}$ . This seems on the low  
 395 side of continental upwelling system estimates of apparent oxygen utilization rates, which  
 396 are between  $1$  and  $5 \mu\text{mol kg}^{-1}\text{d}^{-1}$  (Dortch et al., 1994). So it seems possible the eddy  
 397 has enough exchange with the surrounding water for the residence time to be less than the  
 398 whole time period from late May to September. Note also that during the June cruise, the  
 399 water in the Eddy is slightly cooler than the mixing line, and during the September cruise  
 400 is slightly warmer than the mixing line, so the water in the eddy is evolving seasonally, and  
 401 probably affected by the water temperature in the Vancouver Island Coastal Current, and  
 402 the amount of water getting through the front.

403 The water is mixed enough in the Eddy that it falls along a mixing line, though it  
 404 remains vertically stratified. The amount of homogenization is such that either the mixing is  
 405 very strong, or the water is retained in the eddy for a long time. The amount of turbulence  
 406 required to homogenize 100 m of water over 90 days is  $\kappa \approx 10^{-3} \text{ m}^2\text{s}^{-1}$ . Given that the  
 407 diffusivity implied in the cross-channel surveys was (very) locally on the order of  $\kappa_\rho =$   
 408  $10 \text{ m}^2\text{s}^{-1}$ , this number is not outrageous if we think that such high dissipation is found in  
 409  $10^{-4}$  of the water column. We can more carefully quantify this by considering a synthetic  
 410 profile or temperature and salinity based on an offshore profile, extrapolated from the bottom  
 411 of the 200-m cast to 250 m, assuming that the temperature and salinity at 250 m are  $6.2 [\text{°C}]$   
 412 and 34 psu respectively (figure 15). Water at the offshore station was warmer than onshore,  
 413 so the profile was also linearly interpolated to a surface value of  $(12 \text{ °C}, 31.6 \text{ psu})$ . The profile  
 414 was then linearly compressed into a depth range of 150 m representative of the shelf depth in  
 415 the dense pool, and subjected to mixing with a constant diffusivity of  $\kappa = 10^{-3} \text{ m}^2\text{s}^{-1}$ , with  
 416 the surface and bottom values pinned under the assumption that the near-bottom source  
 417 and surface waters are replenished from a large reservoir. Similar to the naive scaling, the  
 418 T-S relationship does not approach a straight line until after approximately 60-100 days, or  
 419 until the mixing affects a vertical length scale of  $\lambda = (\tau\kappa)^{1/2}$  that is greater than  $\approx 70 \text{ m}$ .

420 The sharpness of the front with the eddy and the offshore water is also intriguing. It  
 421 was persistent for the duration of our detailed survey (figure 8), and, so far as we can tell  
 422 with the limited resolution, was present during the La Perouse cruises. There is not any  
 423 substantial bathymetry blocking the onshore incursion of water at this location, so there  
 424 must be a dynamic barrier. In contrast, numerical simulations of this region reported by  
 425 (Sahu et al., 2022) using a NEMO 36th-degree regional model indicate that there is more  
 426 rapid exchange (order 40 days) between the deep eddy water and the rest of the coastal  
 427 ocean. In this model, the region where the eddy resides has velocities equal or greater than  
 428 other parts of the shelf, and water has an approximate residence time of less than 20 days.  
 429 The eddy water in the model does develop a distinct  $\theta$ -S signature, but not nearly as strong  
 430 as observed. It also has a front with the offshore water, but the front is much wider and  
 431 more gradual than that observed here.

432 Overall, it would be an improvement to our understanding of the eddy if we could  
 433 sample the shelf more persistently. The eddy was already well-formed by the June La  
 434 Perouse cruise, and seems to evolve slowly during that time. Capturing its formation,  
 435 presumably earlier in the spring, and its evolution through the year would be valuable in  
 436 understanding retention and exchange on this productive part of the shelf.

## 437 4.2 Offshore exchange of shelf water

438 The (apparent) displacement of shelf water from La Perouse Bank is a dramatic de-  
 439 parture from geostrophically balanced isobath-following flow.. Eddies have been known to  
 440 separate from irregular coastal topography, both at the surface (Barth et al., 2000), and  
 441 deeper in the water column (Pelland et al., 2013). It has been recognized that instabilities

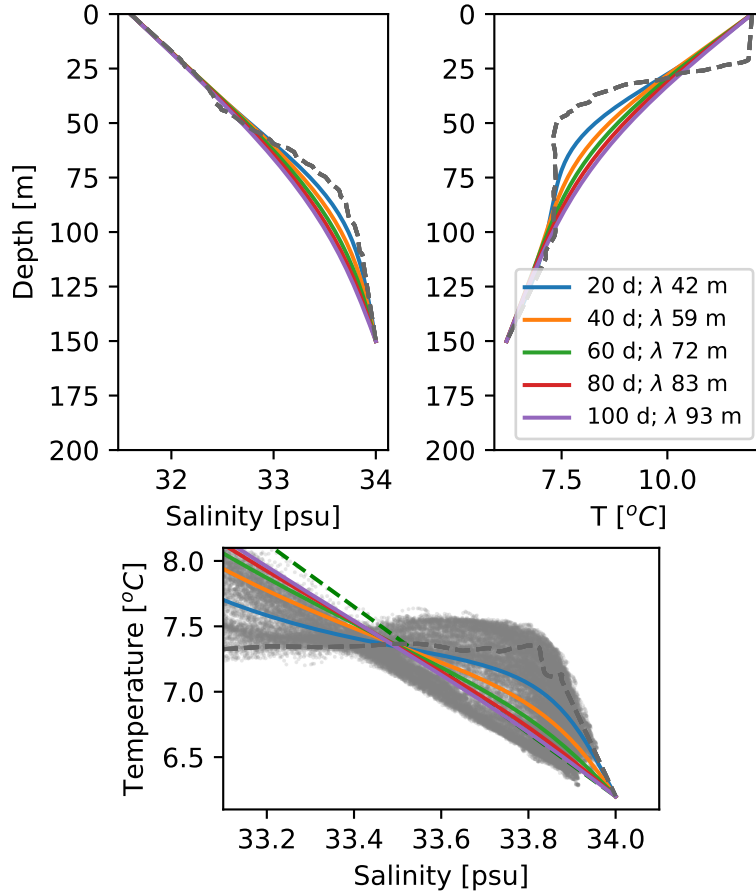


**Figure 15.** Mixing model assuming constant eddy diffusivity of  $\kappa = 10^{-3} \text{ m}^2 \text{s}^{-1}$  acting on an offshore temperature and salinity profiles compressed from 250 thick to 150 m thick. Profiles are pinned to the deep value at (34 psu, 6.2  $^{\circ}$ C), and a shallow one at (31.6 psu, 12  $^{\circ}$ C).

lead to exchange between the open ocean and the shelf at this location (Ikeda & Emery, 1984, 1984). However, observations of the wholesale replacement of shelf water by a new water mass from offshore, is rare. In our situation it is clear that water from as deep as 150 m is separating from the shelf and moving offshore (figure 8, figure 12).

Satellite imagery makes it clear that there is often an exchange between coastal and deepwater along the Vancouver Island shelf (figure 16). Most years there are three or four large excursions from the shelf into the open ocean, many of them over 100 km long. This lengthscale is somewhat larger than 60 km inferred for this region by Ikeda et al. (1984) using a four-layer instability analysis. It is possible that there is even some spatial locking of these features, with a persistent separation at the north tip of the Island, and a strong tendency for one at 49.5 N. Our study area also has evidence of a separation in most of the years, with 2011 being the only clear exception. General baroclinic instability of the upwelling front is a possible mechanism to drive offshore exchange (e.g. Ikeda et al., 1984; Durski & Allen, 2005), but this tends to be shallow, with smaller-scale instabilities that will not extend as far into the interior ocean as observed here. Rather it seems likely that the topographic change engendered by the sudden turn to the east of La Perouse bank catalyses a larger scale instability at this location. In Durski and Allen (2005), when including realistic shelf bathymetry including Heceta Bank, the region around the bank catalyzes intermittent large-scale instabilities similar to the feature here and along the coast (Battieen, 1997).

Large-scale mixing between the shelf and open ocean has been evident since the satellite era. Here we demonstrate that in this study area the flow is originating on the shelf and separating from the bathymetry and being injected into the interior down to the bottom of the water column. A similar observation was made by Barth et al. (2000) downstream of Cape Blanco, Oregon, where the coastal current was observed to detach from the shelf in the lee of the cape, and flow into the interior. They hypothesized that as the current moved offshore, it deepened, stretching isopycnals and creating cyclonic relative vorticity that would tend to push the current back onshelf, but then it was caught in the undercurrent and stalled, being pushed offshore. It is also possible that coastally trapped waves in the region experience a hydraulic control, and these meanders are the response (Dale & Barth, 2001).

Regardless of the dynamics, the offshore transport is substantial. If we assume the coastal current is approximately  $0.1 \text{ m s}^{-1}$  over 100 m in the vertical and 20 km in the horizontal, it represents 0.2 Sv of nutrient- and chlorophyll-rich shelf water transported offshore. Our observations are a finer detailed representation of the kind of cross-shore transports inferred by Mackas and Yelland (1999) from hydrographic surveys, and definitively show that this water can originate from the shelf from relatively deep depths and be transported offshore. We do not have velocity measurements for the water that replaces it, but assuming that water also flows along-shelf, there is a large replacement of shelf water with offshore water at this location. This emphasizes the importance of three dimensional observations and modeling of cross-shelf dynamics when thinking about biological processes on the shelf.

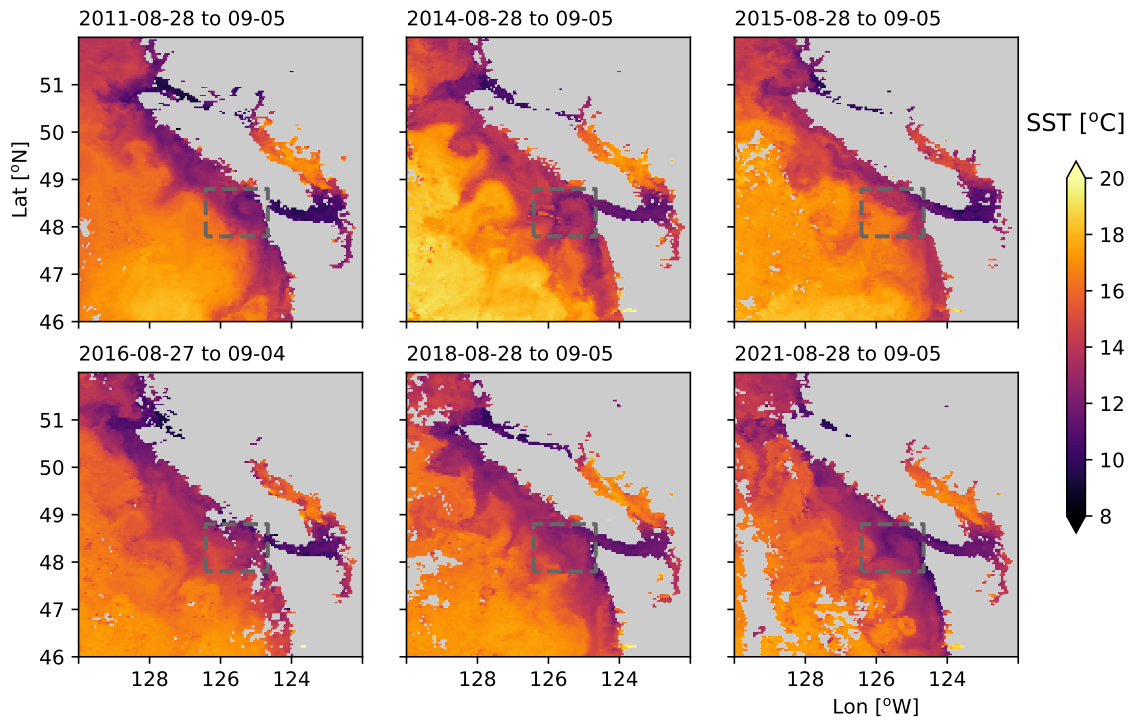


**Figure 16.** Available late-August sea-surface temperature from 8-day composites, 2011 to 2021 (NASA Ocean Biology Processing Group, 2019); missing years had too much cloud cover or no satellite coverage.

482 **Open Research**483 **Acknowledgments**

484 This section is optional. Include any Acknowledgments here.

485 **References**

- Barth, J. A., Pierce, S. D., & Smith, R. L. (2000). A separating coastal upwelling jet at Cape Blanco, Oregon and its connection to the California Current system. *Deep Sea Res. II*, 47(5–6), 783 - 810. doi: [http://dx.doi.org/10.1016/S0967-0645\(99\)00127-7](http://dx.doi.org/10.1016/S0967-0645(99)00127-7)
- Batteen, M. L. (1997). Wind-forced modeling studies of currents, meanders, and eddies in the California Current system. *J. Geophys. Res.*, 102(C1), 985–1010. doi: [10.1029/96jc02803](https://doi.org/10.1029/96jc02803)
- Brink, K. (2016). Cross-shelf exchange. *Annu. Rev. Mar. Sci.*, 8(1), 59–78. doi: [10.1146/annurev-marine-010814-015717](https://doi.org/10.1146/annurev-marine-010814-015717)
- Castelao, R. M., & Barth, J. A. (2007, nov). The role of wind stress curl in jet separation at a cape. *J. Phys. Oceanogr.*, 37(11), 2652–2671. doi: [10.1175/2007jpo3679.1](https://doi.org/10.1175/2007jpo3679.1)
- Dale, A. C., & Barth, J. A. (2001, jan). The hydraulics of an evolving upwelling jet flowing around a cape. *Journal of Physical Oceanography*, 31(1), 226–243. doi: [10.1175/1520-0485\(2001\)031\(0226:thoaeu\)2.0.co;2](https://doi.org/10.1175/1520-0485(2001)031(0226:thoaeu)2.0.co;2)
- Dewey, R. K., & Crawford, W. R. (1988). Bottom stress estimates from vertical dissipation rate profiles on the continental shelf. *J. Phys. Oceanogr.*, 18, 1167–1177.
- DFO. (2022). *Marine environmental data section archive, buoy c46206*. Ecosystem and Oceans Science, Department of Fisheries and Oceans Canada. Retrieved 2022-01-31, from <https://meds-sdmm.dfo-mpo.gc.ca>
- Dortch, Q., Rabalais, N. N., Turner, R. E., & Rowe, G. T. (1994, dec). Respiration rates and hypoxia on the Louisiana shelf. *Estuaries*, 17(4), 862. doi: [10.2307/1352754](https://doi.org/10.2307/1352754)
- Durski, S. M., & Allen, J. S. (2005). Finite-amplitude evolution of instabilities associated with the coastal upwelling front. *J. Phys. Oceanogr.*, 35(9), 1606–1628. doi: [10.1175/jpo2762.1](https://doi.org/10.1175/jpo2762.1)
- Engida, Z., Monahan, A., Ianson, D., & Thomson, R. E. (2016). Remote forcing of subsurface currents and temperatures near the northern limit of the California Current system. *J. Geophys. Res.*, 121(10), 7244–7262. doi: [10.1002/2016jc011880](https://doi.org/10.1002/2016jc011880)
- Foreman, M. G. G., Callendar, W., MacFadyen, A., Hickey, B. M., Thomson, R. E., & Lorenzo, E. D. (2008). Modeling the generation of the Juan de Fuca Eddy. *J. Geophys. Res.*, 113(C3). doi: [10.1029/2006jc004082](https://doi.org/10.1029/2006jc004082)
- Freeland, H., & Denman, K. (1982). A topographically controlled upwelling ceter off southern Vancouver Island. *J. Mar. Res.*, 40(4), 1069–1093.
- Freeland, H., & McIntosh, P. (1989). The vorticity balance on the southern British Columbia continental shelf. *Atmosphere–Ocean*, 27(4), 643–657.
- Hickey, B., Thomson, R., Yih, H., & LeBlond, P. (1991). Velocity and temperature fluctuations in a buoyancy-driven current off Vancouver Island. *J. Geophys. Res.*, 96(C6), 10,507–10,538.
- Hu, C., Lee, Z., & Franz, B. (2012). Chlorophyll a algorithms for oligotrophic oceans: A novel approach based on three-band reflectance difference. *J. Geophys. Res.*, 117(C1). doi: [10.1029/2011jc007395](https://doi.org/10.1029/2011jc007395)
- Ikeda, M., & Emery, W. J. (1984). A continental shelf upwelling event off Vancouver Island as revealed by satellite infrared imagery. *J. Mar. Res.*, 42(2), 303–317. doi: [10.1357/002224084788502774](https://doi.org/10.1357/002224084788502774)
- Ikeda, M., Mysak, L. A., & Emery, W. J. (1984). Observation and modeling of satellite-sensed meanders and eddies off Vancouver Island. *J. Phys. Oceanogr.*, 14(1), 3–21. doi: [10.1175/1520-0485\(1984\)014<0003:omso>2.0.co;2](https://doi.org/10.1175/1520-0485(1984)014<0003:omso>2.0.co;2)
- Klymak, J. M., Shearman, R. K., Gula, J., Lee, C. M., D'Asaro, E. A., Thomas, L. N., ... others (2016). Submesoscale streamers exchange water on the north wall of the Gulf

- 533 Stream. *Geophys. Res. Lett.*. doi: 10.1002/2015GL067152
- 534 MacFadyen, A., & Hickey, B. M. (2010). Generation and evolution of a topographically  
535 linked, mesoscale eddy under steady and variable wind-forcing. *Cont. Shelf Res.*,  
536 30(13), 1387–1402. doi: 10.1016/j.csr.2010.04.001
- 537 Mackas, D. L., Denman, K. L., & Bennett, A. F. (1987). Least squares multiple tracer  
538 analysis of water mass composition. *J. Geophys. Res.*, 92(C3), 2907–2918.
- 539 Mackas, D. L., & Yelland, D. R. (1999, nov). Horizontal flux of nutrients and plankton  
540 across and along the British Columbia continental margin. *Deep Sea Res. II*, 46(11–  
541 12), 2941–2967. doi: 10.1016/s0967-0645(99)00089-2
- 542 NASA Ocean Biology Processing Group. (2017). *MODIS-aqua level 3 mapped chloro-*  
543 *phyll data version r2018.0*. NASA Ocean Biology DAAC. Retrieved from <https://oceancolor.gsfc.nasa.gov/data/10.5067/AQUA/MODIS/L3M/CHL/2018> doi: 10  
544 .5067/AQUA/MODIS/L3M/CHL/2018
- 545 NASA Ocean Biology Processing Group. (2019). *MODIS-aqua level 3 mapped SST data*  
546 *version r2019.0*. NASA Ocean Biology DAAC. Retrieved from [https://oceandata.sci.gsfc.nasa.gov/ob/getfile/AQUA\\_MODIS](https://oceandata.sci.gsfc.nasa.gov/ob/getfile/AQUA_MODIS)
- 547 OSI SAF. (2015). *GHRSST level 2p sub-skin sea surface temperature from the Advanced*  
548 *Very High Resolution Radiometer (AVHRR) on Metop satellites (currently Metop-A)*  
549 *(GDS V2) produced by OSI SAF*. NASA Physical Oceanography DAAC. Retrieved  
550 from [https://podaac.jpl.nasa.gov/dataset/AVHRR\\_SST\\_METOP\\_A-OSISAF-L2P-v1.0](https://podaac.jpl.nasa.gov/dataset/AVHRR_SST_METOP_A-OSISAF-L2P-v1.0) doi: 10.5067/GHAMA-2PO02
- 551 Pelland, N. A., Eriksen, C. C., & Lee, C. M. (2013). Subthermocline eddies over the  
552 washington continental slope as observed by seagliders, 2003–09. *J. Phys. Oceanogr.*  
553 doi: 10.1175/JPO-D-12-086.1
- 554 Relvas, P., & Barton, E. D. (2005). A separated jet and coastal counterflow during upwelling  
555 relaxation off Cape São Vicente (Iberian Peninsula). *Cont. Shelf Res.*, 25(1), 29–49.  
556 doi: 10.1016/j.csr.2004.09.006
- 557 Sahu, S., Allen, S. E., Saldías, G. S., Klymak, J. M., & Zhai, L. (2022, mar). Spatial and  
558 temporal origins of the La Perouse low oxygen pool: A combined lagrangian statistical  
559 approach. *J. Geophys. Res.*, 127(3). doi: 10.1029/2021jc018135
- 560 Thomson, R. E., & Gower, J. F. R. (1998, feb). A basin-scale oceanic instability event in  
561 the gulf of alaska. *J. Geophys. Res.*, 103(C2), 3033–3040. doi: 10.1029/97jc03220
- 562 Thomson, R. E., Hickey, B. M., & LeBlond, P. H. (1989). The Vancouver Island Coastal  
563 Current: Fisheries barrier and conduit. In R. J. Beamish & G. A. McFarlane (Eds.),  
564 *Effects of ocean variability on recruitment and an evaluation of parameters used in*  
565 *stock assessment models*. Fisheries and Oceans Canada.
- 566 Thomson, R. E., & Krassovski, M. V. (2015, dec). Remote alongshore winds drive variability  
567 of the California Undercurrent off the British Columbia–Washington coast. *J. Geophys.*  
568 *Res.*, 120(12), 8151–8176. doi: 10.1002/2015jc011306
- 569 Weaver, A. J., & Hsieh, W. W. (1987). The influence of buoyancy flux from estuaries  
570 on continental shelf circulation. *J. Phys. Oceanogr.*, 17, 2127–2140. doi: 10.1175/  
571 1520-0485(1987)017<2127:TIOBFF>2.0.CO;2